

Supplemental Information

Unveiling the New Function of Uranyl Molecular Clusters as a Fluorometric Sensor for UV and X-ray Dosimetry

Huangjie Lu ^{b,c}, Zhaofa Zheng ^{b,c}, Yuan Qian ^{b,c}, Jian-Qiang Wang ^{b,c, *}, Jian Lin ^{a, *}

* Jian-Qiang Wang.

E-mail address: wangjianqiang@sinap.ac.cn

* Jian Lin.

E-mail address: jianlin@xjtu.edu.cn

Table of Contents

Table of Contents	2
S1. Experimental Procedures.....	3
S1.1 Materials and Synthesis.....	3
S1.2 Characterizations	3
S2. Supplemental Figures and Tables.....	5
Fig. S1. The nearest π - π distances of phen ligands in 1 and 2.	5
Fig. S2. (a) The FTIR spectra of phen and 1 (before and after irradiation with UV, X-ray, and γ -ray). (b) The FTIR spectra of phen and 2 (inset: FTIR spectrum of 2 ranging from 700 to 1400 cm^{-1}).	5
Fig. S3. Luminescence spectra of 1, 2, and phen under 365 nm UV excitation.	6
Fig. S4. The baseline intensity of blank sample in dark.	6
Fig. S5. Luminescence spectra of 1 upon alternative X-ray irradiation and heating treatments.	7
Fig. S6. The theoretical and experimental PXRD patterns of 1 before and after irradiation with UV, X-, and γ -ray.....	7
Fig. S7. The stability measurement of radiation-induced radicals. The inset shows the luminescence spectra before irradiation, after irradiation (2h), and after being stored in dark for 0, 1, 3, 7, 12, and 24 h.	8
Fig. S8. PXRD patterns of (a) 1 and (b) 2 treated with different relative humidity (RH) conditions (35%, 65%, and 95%).....	8
Fig. S9. Temperature-dependent PXRD patterns of (a) 1 and (b) 2 showing that the structure of 1 remains unchanged upon heating to 290 $^{\circ}\text{C}$	9
Fig. S10. Thermogravimetric curves of 1 and 2.	9
Table S1. Crystallographic data of 1 and 2.....	10
Table S2. Bond valent sum (BVS) analysis on 2.....	10
Table S3. Selected bond lengths and bond angles of 1.....	11
Table S4. Selected bond lengths and bond angles of 2.....	11
S3. References	12

S1. Experimental Procedures

S1.1 Materials and Synthesis

Caution! All uranium compounds used and investigated were operated in an authorized laboratory designed for actinide element studies. Standard protections for radioactive materials should be followed.

Materials. All reagents were purchased from chemical reagent suppliers and used without further purification. $\text{UO}_2(\text{NO}_3)_2 \cdot 5\text{H}_2\text{O}$ (99.99%), $\text{UO}_2(\text{CH}_3\text{COO})_2 \cdot 2\text{H}_2\text{O}$ (99.99%), $\text{Eu}(\text{NO}_3)_3 \cdot 6\text{H}_2\text{O}$ (99.99%, Aladdin Co.), and 1,10-phenanthroline monohydrate (phen, 99.99%, Aladdin Co.).

Synthesis. For **1**, $\text{UO}_2(\text{CH}_3\text{COO})_2 \cdot 2\text{H}_2\text{O}$ (0.1 mmol, 0.0424 g) and phen (0.1 mmol, 0.0198 g) were charged into a 5 mL vial and then dissolved in 2 mL deionized water. Subsequently, the samples were sealed and heated at 100 °C for 1 day. For **2**, $\text{UO}_2(\text{NO}_3)_2 \cdot 5\text{H}_2\text{O}$ (0.1 mmol, 0.0502 g), $\text{Eu}(\text{NO}_3)_3 \cdot 6\text{H}_2\text{O}$ (0.1 mmol, 0.0446 g), and phen (0.1 mmol, 0.0198 g) were charged into a 5 mL vial and then dissolved using 1 mL deionized water and 1 mL DMF. Subsequently, the samples were sealed and heated at 90 °C for 1 day. The single crystals **1** and **2** were washed by deionized water and ethanol, and then dried at room temperature.

S1.2 Characterizations

Crystallographic Analysis. Single-crystal XRD data **1** and **2** were collected on a Bruker D8-Venture single-crystal X-ray diffractometer equipped with an I μ S 3.0 microfocus X-ray source (Mo-K α radiation, $\lambda = 0.71073 \text{ \AA}$) and a CMOS detector at 298 K. The data frames were collected using the *APEX3* program and processed using the *SAINTE* routine. The empirical absorption correction was applied using the *SADABS* program.¹ The structure was solved by Intrinsic Phasing with *ShelXT*² and refined with *ShelXL*³ using *OLEX2*⁴. All the non-H atoms were subjected to anisotropic refinement by full-matrix program and refined with a full-matrix least-squares technique. Anisotropic thermal parameters were applied to all nonhydrogen atoms. Contributions to scattering due to these highly disordered solvent molecules were removed in **2** using the *SQUEEZE* routine of *PLATON*.^{3,5} Structures were then refined again using the data generated.

Powder X-ray diffraction (PXRD). Data were collected from 5 to 50° with a step of 0.02° and the time for data collection was 0.2–0.5 s on a Bruker D8 Advance diffractometer with Cu K α radiation ($\lambda = 1.54056 \text{ \AA}$) and a Lynxeye one-dimensional detector.

Luminescence Spectroscopy. The single crystal solid-state luminescence spectra were recorded on a Craic Technologies microspectrophotometer. Crystals were placed on quartz slide, and data was collected after auto-set optimization. When the 365 nm excitation light (2mW) was selected, an optical filter masking signal below 420 nm was applied in order to mask the interference of excitation light.

Fourier Transform Infrared Spectroscopy. The FTIR spectra were recorded in the range of 400–4000 cm^{-1} using a Thermo Nicolet 6700 FTIR spectrometer equipped with a diamond attenuated total reflectance (ATR) accessory.

Thermalgravimetric Analysis (TGA). TGA was carried out in an N_2 atmosphere with a heating rate of 10 $^{\circ}\text{C}/\text{min}$ from 30 to 900 $^{\circ}\text{C}$ on a NETZSCH STA 449 F3 Jupiter instrument.

Electron Paramagnetic Resonance (EPR) Study. The electron paramagnetic resonance (EPR) measurements were performed on a JEOL-FA200 spectrometer at the X-band with 100 kHz field modulation. The EPR spectra of nonirradiated and irradiated samples were recorded at room temperature and the microwave power used was 1.0 mW.

Radiolytic Stability. The radiation resistance was examined by irradiating the powdery sample with UV, X-ray, or γ -ray. X-ray and γ -ray were provided by a $\text{Cu K}\alpha$ radiation source (60 kV, 12W) and a ^{60}Co irradiation source (2.22×10^{15} Bq), respectively. **1** was irradiated with X-ray and γ -ray with dose rates of 7.2 and 11.8 kGy/h, respectively. PXRD, FTIR, and SCXRD analyses on the irradiated samples were performed to confirm the radiation resistance of **1**.

S2. Supplemental Figures and Tables

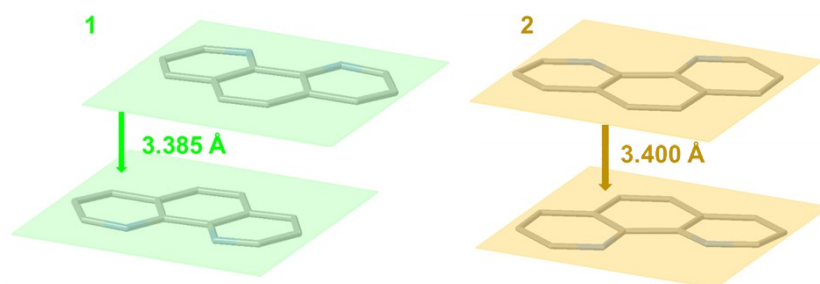


Fig. S1. The nearest π - π distances of phen ligands in **1** and **2**.

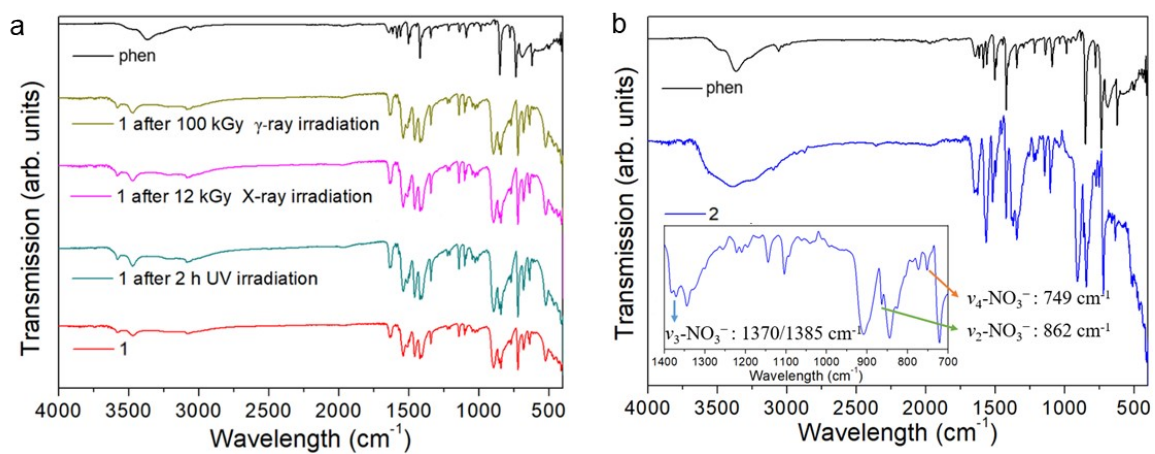


Fig. S2. (a) The FTIR spectra of phen and **1** (before and after irradiation with UV, X-ray, and γ -ray). (b) The FTIR spectra of phen and **2** (inset: FTIR spectrum of **2** ranging from 700 to 1400 cm^{-1}).

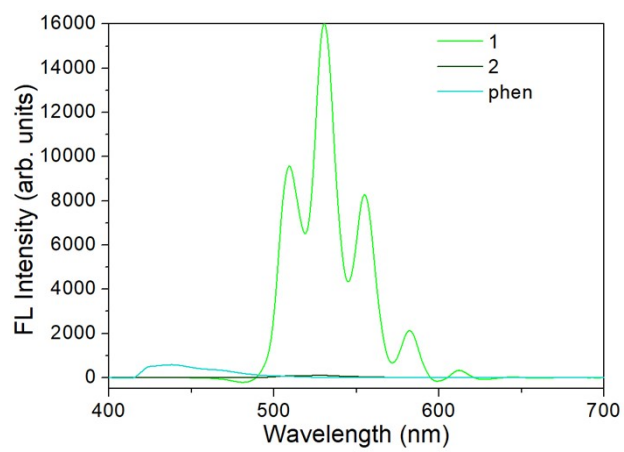


Fig. S3. Luminescence spectra of **1**, **2**, and phen under 365 nm UV excitation.

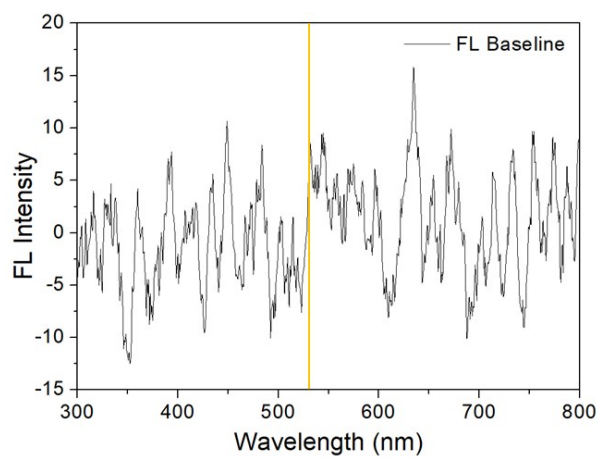


Fig. S4. The baseline intensity of blank sample in dark.

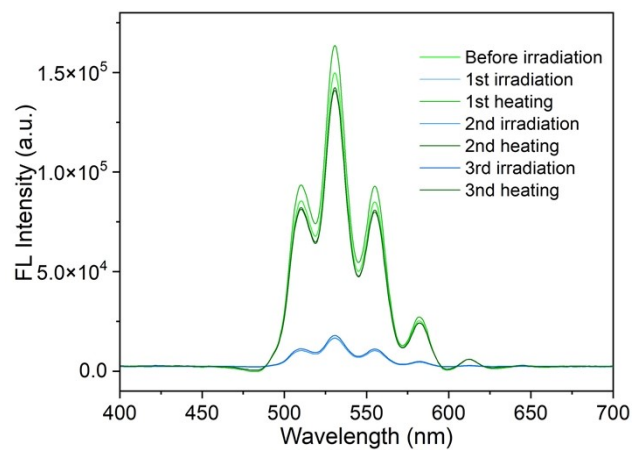


Fig. S5. Luminescence spectra of **1** upon alternative X-ray irradiation and heating treatments.

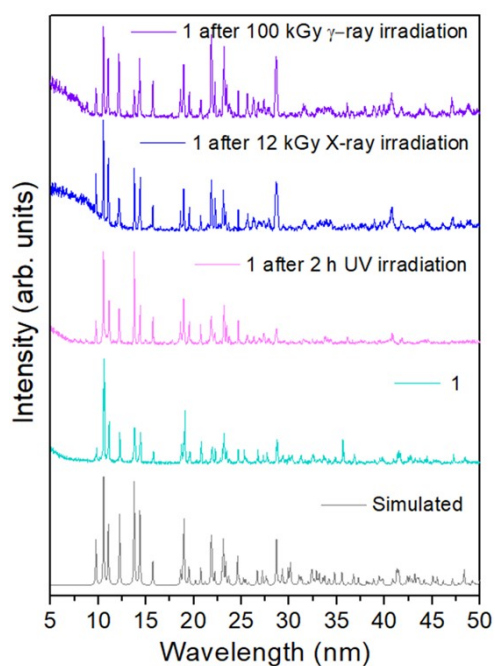


Fig. S6. The theoretical and experimental PXRD patterns of **1** before and after irradiation with UV, X-, and γ -ray.

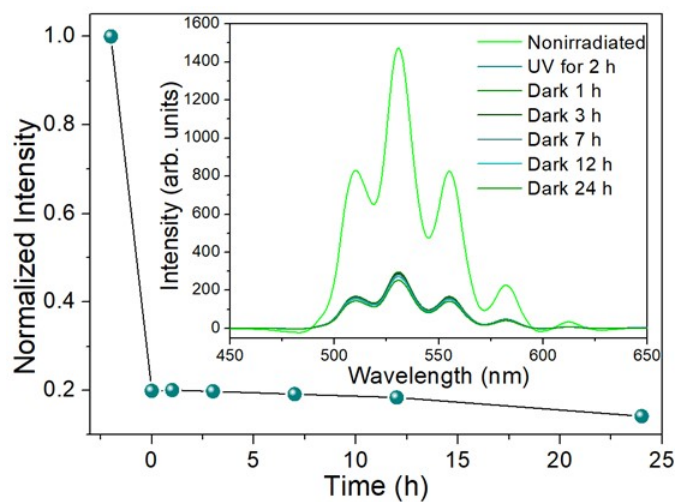


Fig. S7. The stability measurement of radiation-induced radicals. The inset shows the luminescence spectra before irradiation, after irradiation (2h), and after being stored in dark for 0, 1, 3, 7, 12, and 24 h.

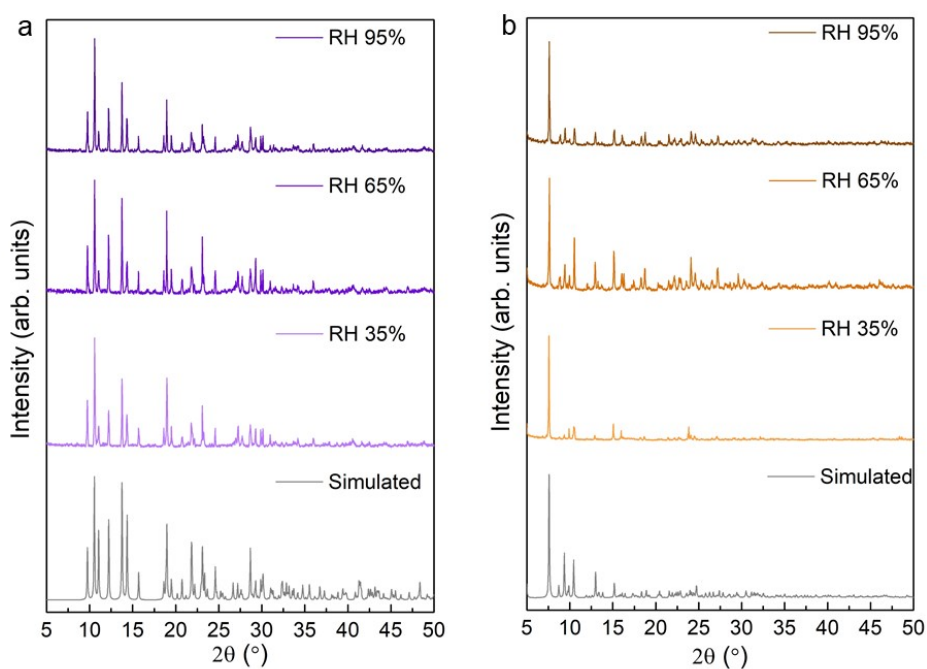


Fig. S8. PXRD patterns of (a) **1** and (b) **2** treated with different relative humidity (RH) conditions (35%, 65%, and 95%).

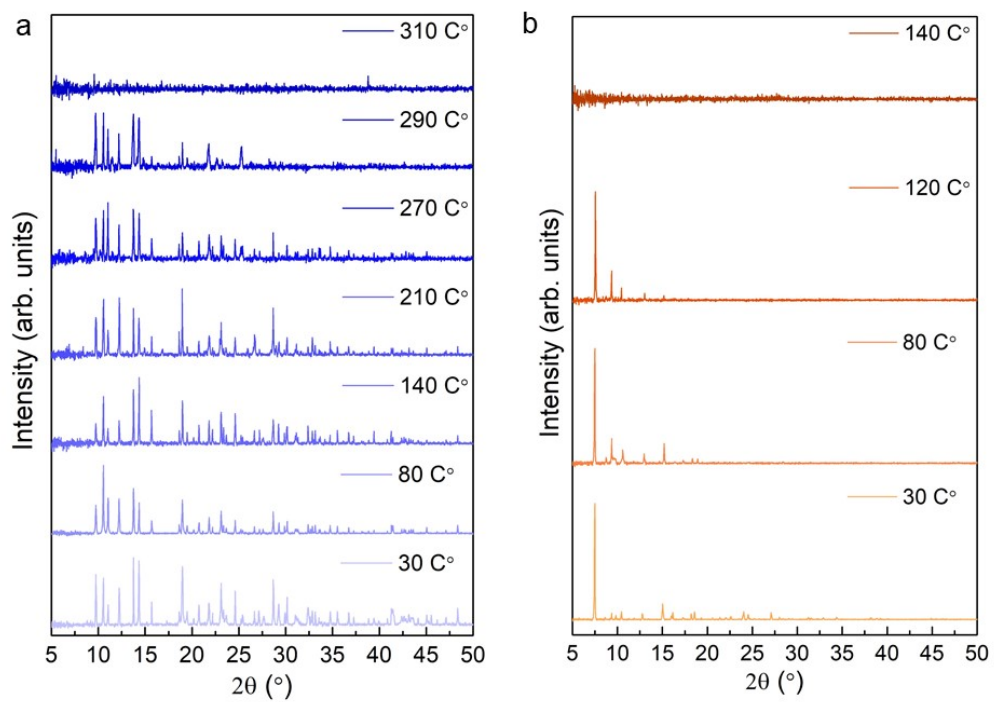


Fig. S9. Temperature-dependent PXRD patterns of (a) **1** and (b) **2** showing that the structure of **1** remains unchanged upon heating to 290 °C.

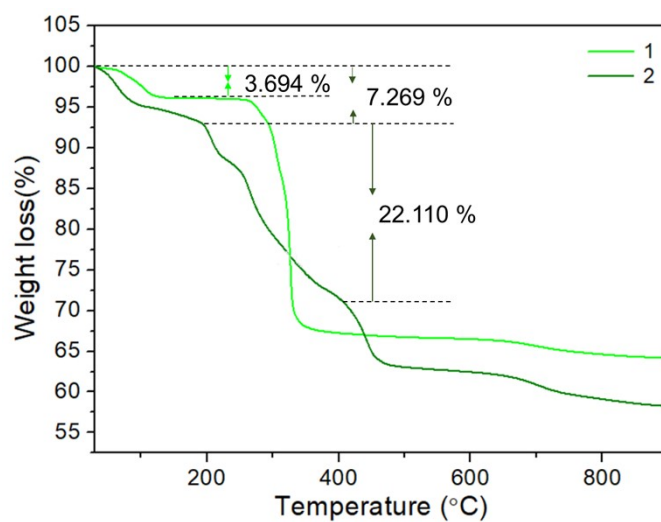


Fig. S10. Thermogravimetric curves of **1** and **2**.

Table S1. Crystallographic data of **1** and **2**.

Compound	1 before irradiation	1 after irradiation	2
<i>Mass</i>	1028.38	1028.38	2885.04
Color	Yellow	Yellow	Yellow
Habit	Block	Block	Block
Space group	$P2_1/n$	$P2_1/n$	$P-1$
<i>a</i> (Å)	9.4351(3)	9.4343(17)	11.781(4)
<i>b</i> (Å)	9.1130(3)	9.111(2)	12.086(5)
<i>c</i> (Å)	17.3744(7)	17.414(4)	18.056(7)
α (deg)	90	90	93.371(13)
β (deg)	105.329(1)	105.302(6)	95.937(12)
γ (deg)	90	90	104.737(12)
<i>V</i> (Å ³)	1440.74(9)	1443.8(5)	2463.3(16)
<i>Z</i>	2	2	1
<i>T</i> (K)	293(2)	293(2)	296(2)
λ (Å)	0.71073	0.71073	0.71073
<i>Max 2θ</i> (deg)	55.110	55.114	55.166
ρ_{calcd} (g cm ⁻³)	2.371	2.365	1.945
μ (Mo K α)	0.71073	0.71073	0.71073
<i>R</i> ₁	0.0228	0.0219	0.0360
<i>wR</i> ₂	0.0633	0.0618	0.1068
<i>R</i> _{int}	0.0442	0.0470	0.0515
<i>GOF</i>	1.010	1.023	1.062

Table S2. Bond valent sum (BVS) analysis on **2**.

Atom	BVS	Assignment
U1	5.83	
U2	5.75	
U3	5.76	
O1	1.96	$\mu_3\text{-O}^{2-}$
O2	1.28	$\mu_2\text{-OH}^-$
O4	1.18	$\mu_2\text{-OH}^-$
O3	1.65	
O5	1.68	
O6	1.66	
O7	1.68	
O8	1.70	
O9	1.69	
O10	2.15	
O11	1.96	

Table S3. Selected bond lengths and bond angles of **1**.

Bond length (Å) and bond angle (°)					
Before irradiation			After irradiation		
U=O	U1-O1	1.773(4)	U=O	U1-O1	1.772(4)
	U1-O2	1.766(3)		U1-O2	1.771(3)
U-N/O	U1-N1	2.646(4)	U-N/O	U1-N1	2.649(4)
	U1-N2	2.648(3)		U1-N2	2.643(3)
	U1-O3	2.334(3)		U1-O3	2.340(3)
	U1-O4	2.287(3)		U1-O4	2.291(3)
	U1-O4	2.343(3)		U1-O4	2.341(3)
$\angle O2=U1=O1$		174.83(16)	$\angle O2=U1=O1$		175.03(15)

Table S4. Selected bond lengths and bond angles of **2**.

Bond length (Å) or bond angle (°)		
U=O	U1-O5	1.782(5)
	U1-O8	1.775(5)
	U2-O3	1.792(5)
	U2-O9	1.778(6)
	U3-O6	1.787(5)
	U3-O7	1.782(5)
U-N/O	U1-N2	2.638(6)
	U1-N3	2.641(6)
	U2-N1	2.660(6)
	U2-N5	2.679(6)
	U3-N4	2.635(6)
	U3-N6	2.680(6)
	U1-O1	2.313(5)
	U1-O2	2.310(5)
	U1-O4	2.323(5)
	U2-O1	2.264(5)
	U2-O4	2.328(5)
	U2-O10	2.356(6)
	U3-O1	2.245(5)
	U3-O2	2.354(5)
U3-O11	2.365(6)	
$\angle O5=U1=O8$		174.7(2)
$\angle O3=U2=O9$		176.4(2)
$\angle O6=U3=O7$		175.3(2)

S3. References

1. G. M. Sheldrick, 1996.
2. G. M. Sheldrick, *Acta Crystallogr. Sect. A: Found. Adv.*, 2015, **71**, 3.
3. G. M. Sheldrick, *Acta Crystallogr. Sect. C: Struct. Chem.*, 2015, **71**, 3.
4. O. V. Dolomanov, L. J. Bourhis, R. J. Gildea, J. A. K. Howard and H. Puschmann, *J. Appl. Cryst.*, 2009, **42**, 339.
5. A. L. Spek, *Acta Crystallogr. Sect. C: Struct. Chem.*, 2015, **71**, 9.